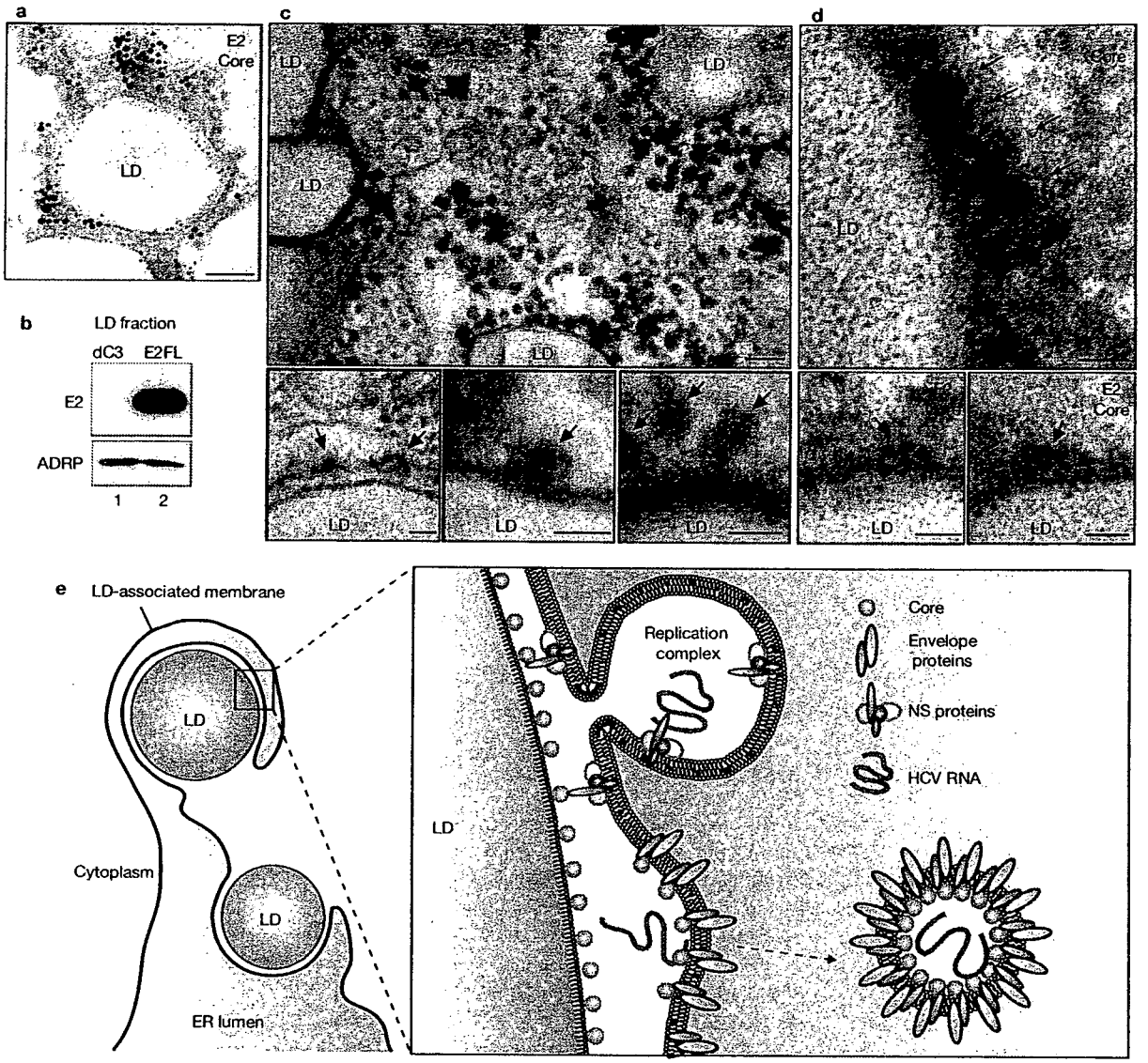

Figure 5 Virus-assembly takes place around the LDs. (**a**) Immunoelectron microscopic detection of E2 and Core in JFH1^{E2FL}-replicating cells. E2 and Core are labelled with 15 nm and 10 nm gold particles, respectively. (**b**) Western blot analysis of the lipid droplet (LD) fraction from JFH1^{E2FL} and JFH1^{dC3} replicon-bearing cells with anti-E2 and anti-ADRP antibodies. (**c**) Transmission electron micrographs of JFH1^{E2FL}-replicating cells. Arrows indicate virus-like particles. (**d**) Immunoelectron micrographs of LDs labelled with antibodies against Core (10 nm) and E2 (15 nm) are shown. Arrows show Core in electron-dense granules. Scale bar: **a** and upper panel of **c**: 100 nm; in **d** and lower panels of **c**: 50 nm. (**e**) A model for the production of infectious hepatitis C virus (HCV). Core mainly localizes on the monolayer membrane that surrounds the LD. HCV induces the apposition of the LD to the endoplasmic reticulum (ER)-derived bilayer membranes (LD-associated membrane). Core recruits NS proteins, as well as replication complexes, to the LD-associated membrane. NS proteins around the LD can then participate in infectious virus production. E2 also localizes around the LD. Through these associations, virion assembly proceeds in this local environment. Uncropped images of gels are shown in Supplementary Information Fig. S6.

larger than that of Core (Fig. 3b). The LD-proximal NS5A signal partially overlapped with the Core signal (Fig. 3b, c, grey). This concentric staining pattern was also observed with the other NS proteins (Supplementary Information, Fig. S5a), indicating that NS proteins associate with Core on the surface of LDs. Electron microscopic analysis only rarely revealed a close association of LDs with other organelles in naïve Huh-7 cells (Fig. 3d, f). However, in the case of JFH1^{E2FL}-replicating cells, about 30% of the LDs were in close proximity to membrane cisternae (Fig. 3e, arrows; 3f), arguing for a HCV-induced membrane rearrangement around LDs. Core was mainly located on the periphery of LDs, and occasionally signals were observed in more distal areas of the LDs (Fig. 3g, arrowheads and arrows, respectively). Although some NS5A signals were observed on the surface of the LD, the majority of NS5A signals were detected more distal of LDs (Fig. 3h, i). Furthermore, we often observed membrane cisternae as white lines in the same area as NS5A signals (Fig. 3i, arrows). When the same section was labelled with anti-Core and anti-NS5A antibodies, Core was detected on the surface of the LDs, whereas NS5A was mainly observed in the peripheral area of the LDs (Fig. 3j, arrowheads and arrows, respectively). In summary, these results show that Core recruits NS proteins, as well as HCV replication complexes, to the LD-associated membranes.

The above results prompted us to ask whether Core–LD colocalization is important for the production of infectious virus particles. JFH1^{E2FL}-replicating cells released virions into the culture medium and these viruses were highly infectious for naïve Huh-7.5 cells[11,21], although culture medium from JFH1$^{PP/AA}$- or JFH1^{dC3}-replicating cells did not contain significant levels of HCV RNA and infectious virus (Fig. 4a). However, following trans-complementation with Core^{Wt}, a high titre of HCV RNA and infectious virus could be rescued from JFH1^{dC3}-replicating cells (Fig. 4b; and see Supplementary Information, Fig. S5b, c). In contrast, the production of infectious viruses was not rescued by trans-complementation with Core$^{PP/AA}$ (Fig. 4b). RNA-binding properties and oligomerization of Core^{Wt} and Core$^{PP/AA}$, which are both necessary for virus assembly, were similar (Supplementary Information, Fig. S5d; ref. 22), arguing that the primary defect of this mutant in preventing infectious virus production is the inability to associate with LDs.

To investigate the contribution of NS proteins around LDs to infectious virus production, we used variants of NS5A, which were not recruited to LDs even in the presence of Core. We assumed that NS5A was crucial for recruiting other NS proteins to LDs, because the level of NS5A recruited to LDs via Core was higher than the levels of the other recruited NS proteins (Fig. 1c, JFH1^{E2FL}). Using alanine-scanning mutagenesis within the NS5A coding region of JFH1^{E2FL}, we generated two mutants, JFH1^{AAA99} and JFH1^{AAA102}, in which the amino-acid sequence APK (aa 99–101 of NS5A) or PPT (aa 102–104 of NS5A) was replaced by AAA (Supplementary Information, Fig. S1). In JFH1^{AAA99}- and JFH1^{AAA102}-replicating cells, NS5A was rarely detected around LDs, whereas Core was still localized to LDs (Fig. 4c, d). Importantly, these mutations impaired not only the NS5A association with LDs, but also the recruitment of other NS proteins and viral RNAs to LDs (Fig. 4d). These results indicate that NS5A is a key protein that recruits replication complexes to LDs. Importantly, HCV RNA synthesis activity in the LD fractions from these mutant JFH1-replicating cells was also severely impaired (Fig. 4e), corroborating the lack of association of HCV replication complexes with LDs.

To investigate the infectious virus production of these NS5A mutants, we prepared cells expressing similar levels of HCV proteins and RNA by adjusting the amount of transfected HCV RNA (Fig. 4e). This was necessary, because replication activities of these mutants were lower compared with JFH1^{E2FL}. Under these conditions, the amounts of Core and HCV RNA that were released into the culture medium from cells transfected with the mutants were comparable to JFH^{E2FL} (Fig. 4f, upper graph). However, infectivity titres of the mutants were severely reduced (Fig. 4f, lower panels). In sucrose density-gradient centrifugation of culture medium from JFH1^{E2FL}-bearing cells, two types of HCV particles were detected: low-density particles (about 1.12 g ml^{-1}) with high infectivity (Fig. 4g, green area of JFH1^{E2FL}), and high-density particles (about 1.15 g ml^{-1}) without infectivity (yellow area). This result indicates that only a minor portion of released HCV particles is infectious, whereas the majority of released particles lack infectivity. In contrast, cells bearing the JFH1^{AAA99} mutant almost exclusively released non-infectious particles of around 1.15 g ml^{-1}, whereas infectious particles were barely detectable (Fig. 4g, JFH1^{AAA99}). Taken together, these results provide convincing evidence that the association of NS proteins and replication complexes around LDs is critical for producing infectious viruses, whereas production of non-infectious viruses seems to follow a different pathway.

The results described so far imply that some step(s) of HCV assembly take place around LDs. To explore this possibility, we analysed the distribution of the major envelope protein E2 around the LD. Electron microscopic analysis revealed that, in about 90% of JFH1^{E2FL}-replicating cells, E2 was localized in the peripheral area of the LDs (Fig. 5a, large grains). This labelling pattern was similar to the one observed for NS5A (Fig. 3j), indicating that E2 also localizes on the LD-associated membranes. Western blot analysis of the LD fraction supported this conclusion, because the LD fraction that was purified from JFH1^{E2FL}-replicating cells, but not from JFH1^{dC3}-replicating cells, contained E2 (Fig. 5b). Furthermore, spherical virus-like particles with an average diameter of about 50 nm were observed around LDs in JFH1^{E2FL}-replicating cells (Fig. 5c, upper panel). These particles were never observed in naïve Huh-7 cells. A more refined analysis indicates that these particles are closely associated with membranes in close proximity to LDs (Fig. 5c, lower panels, arrows). Finally, these particles around the LDs reacted with Core- and E2-specific antibodies, arguing that the particles represent true HCV virions (Fig. 5d). These results suggest that infectious HCV particles are generated from the LD-associated membranous environment.

In this study, we have demonstrated that Core recruits NS proteins, HCV RNAs and the replication complex to LD-associated membranes. Mutations of Core and NS5A (Fig. 4), which failed to associate with LDs, impaired the production of infectious virus. We note that the mutant Core retains the ability to interact with RNA (Supplementary Information, Fig. S5b) and to assemble into nucleocapside[22]. Similarly, the NS5A mutant still supports viral genome replication and the formation of capsids or virus-like particles, arguing that the introduced mutations in Core and NS5A do not affect overall protein folding, stability or function (Fig. 4). Taken together, the data show that the association of HCV proteins with LDs is important for the production of infectious viral particles (Fig. 5e).

Our results also indicate that NS proteins around the LDs participate in the assembly of infectious virus particles. In one scenario, NS proteins may indirectly contribute to the different steps of virus production — for example, by establishing the microenvironment around the LDs that is required for infectious virus production. Alternatively, NS proteins around the LDs may directly participate in virus production — for example, as components of the replication complex that provide the RNA genome to the assembling nucleocapsid.

In support of the role of LDs in virus formation, we observed that colocalization of HCV protein with LDs was low in cases of the chimera Jc1, supporting up to 1,000-fold higher infectivity titres compared with JFH1 (ref. 13). In a Jc1-infected cell, only about 20% of LDs demonstrated detectable colocalization with Core, but this value increased to 80% in the case of a Jc1 mutant lacking most of the envelope glycoprotein genes and thus being unable to produce infectious virus particles (data not shown). This inverse correlation between the efficiency of virus production and Core protein accumulation on LDs indicates that rapid assembly and virus release results in the rapid liberation of HCV proteins from the LDs.

Steatosis and abnormal lipid metabolism caused by chronic HCV infection may be linked to enhanced LD formation[14]. In fact, the overproduction of LDs is induced by Core (Supplementary Information, Fig. S3) and HCV also induces membrane rearrangements around LDs (Fig. 3d–f). Our findings suggest that excessive Core-dependent formation of LDs

and membrane rearrangements are required to supply the necessary microenvironment for virus production. NS proteins and HCV RNA seem to be translocated from the ER to the LD-associated membranes. Interestingly, the LD-associated membranes were occasionally found in continuity with ribosome-studded rough ER (Fig. 3e, arrowheads). Thus, at least parts of the LD-associated membranes are likely to be derived from ER membranes. ER marker proteins, however, were not detected in the LD fraction, suggesting that the LD-associated membrane is characteristically distinct from that of ER membranes.

To our knowledge, this is the first report showing that LDs are required for the formation of infectious virus particles. The fact that capsid protein of the hepatitis G virus also localizes to LDs[15] indicates that LDs might be important for the production of other viruses as well. Our findings demonstrate a novel function of LDs, provide an important step towards elucidating the mechanism of HCV virion production and open new avenues for novel antiviral intervention. □

METHODS

Antibodies. The antibodies used for immunoblotting and immunolabelling were specific for Core (#32-1 and RR8); E2 (AP-33 (ref. 23); 3/11, CBH5 and Flag M2 (Sigma-Aldrich, St Louis, MO); NS3 (R212)[17]; NS4A and 4B (PR12); NS5A (NS5ACL1); NS5B (NS5B-6 and JFH1-1)[24]; ADRP (Progen Biotechnik, Heidelberg, Germany); tubulin (Oncogene Research Products, MA, USA); Grp78 (StressGen, Victoria, Canada); PDI (StressGen); and Calnexin-NT (StressGen). Antibodies specific for Core (#32-1 and RR8), NS3 (R212) and NS4AB (PR12) were gifts from Dr Kohara (The Tokyo Metropolitan Institute of Medical Science, Japan). Anti-E2 antibody (AP-33) was provided by Dr Patel (MRC Virology Unit, UK). Anti-NS5B (NS5B-6) antibody was kindly provided by Dr Fukuya (Osaka University, Japan). Rabbit polyclonal antibodies specific for NS5A were raised against a bacterially expressed GST–NS5A (1–406 aa) fusion protein. In the case of the HCV chimeras Con1/C3 and H77/C3, immunofluorescence analyses were performed by using the following antibodies: Core (C7/50)[5], a JFH1 NS3-specific rabbit polyclonal antiserum; NS4B (#86)[25]; and NS5A (Austral Biologicals, San Ramon, CA).

Indirect immunofluorescence analysis. Indirect immunofluorescence analysis was performed essentially as described previously[17], with slight modifications. Cells transfected with JFH1 RNA were seeded onto a collagen-coated Labtech II 8-well chamber (Nunc, NY, USA). The coating with collagen was performed using rat-tail collagen type I (BD Bioscience, Palo Alto, CA) according to manufacturer's instructions. Three days after seeding, the cells were washed twice with phosphate-buffered saline (PBS; 137 mM NaCl, 2.7 mM KCl, 4.3 mM Na_2HPO_4 and 1.4 mM KH_2PO_4) and fixed with fixation solution (4% paraformaldehyde and 0.15 M sodium cacodylate at pH 7.4) for 15 min at room temperature. After washing with PBS, the cells were permeabilized with 0.05% Triton X-100 in PBS for 15 min at room temperature. For the precise localization of the proteins, the cells were permeabilized with 50 μg ml^{-1} of digitonin in PBS for 5 min at room temperature[26]. After incubating the cells with blocking solution (10% fetal bovine serum and 5% bovine serum albumin (BSA) in PBS) for 30 min, the cells were incubated with the primary antibodies. The fluorescent secondary antibodies were Alexa 568- or Alexa 647-conjugated anti-mouse or anti-rabbit IgG antibodies (Invitrogen, Carlsbad, CA). Nuclei were labelled with 4',6-diamidino-2-phenylindole (DAPI). LDs were visualized with BODIPY 493/503 (Invitrogen). Analyses of JFH1 were performed on a Leica SP2 confocal microscope (Leica, Heidelberg, Germany). Analysis of the Con1/C3 and the H77/C3 chimeras was performed in the same way, except that imaging was performed on a Nikon C1 confocal microscope (Nikon, Tokyo, Japan).

Electron microscopy. For conventional electron microscopy, cells cultured in plastic Petri dishes were processed *in situ*. The cells were fixed in 2.5% glutaraldehyde and 0.1 M sodium phosphate (pH 7.4), and then in OsO_4 and 0.1 M sodium phosphate (pH 7.4). The cells were then dehydrated in a graded ethanol series and embedded in an epoxy resin. Ultrathin sections were cut perpendicular to the base of the dish. For immuno-electron microscopy, cells were detached from the dish with a cell scraper after fixation in 4% paraformaldehyde, 0.1% glutaraldehyde and 0.1 M sodium phosphate (pH 7.4) for 24 h, and washed in 0.1 M lysine, 0.1 M sodium phosphate (pH 7.4) and 0.15 M sodium chloride. After dehydrating the cells in a graded series of cold ethanol, they were embedded in Lowicryl K4M at −20 °C. Ultrathin sections were labelled with primary antibodies and colloidal gold particles (15 nm) conjugated to anti-mouse IgG or anti-rabbit IgG antibodies. For double labelling, colloidal gold particles with different diameters (10 nm and 15 nm) conjugated to anti-mouse IgG or anti-rabbit antibodies were used. Samples were observed after staining with uranyl acetate and lead citrate with a JEM 1010 electron microscope at the accelerating voltage of 80 kV. Anti-Core (#32-1 and RR88), anti-NS5A (NS5ACL1) and anti-E2 (Flag M2) antibodies were used.

Preparation of the lipid droplets. Cells at a confluency of ~80% on a dish with a diameter of 14 cm were scraped in PBS. The cells were pelleted by centrifugation at 1,500 rpm. The pellet was resuspended in 500 μl of hypotonic buffer (50 mM HEPES, 1 mM EDTA and 2 mM $MgCl_2$ at pH 7.4) supplemented with protease inhibitors (Roche Diagnostics, Basel, Switzerland) and was incubated for 10 min at 4 °C. The suspension was homogenized with 30 strokes of a glass Dounce homogenizer using a tight-fitting pestle. Then, 50 μl of 10× sucrose buffer (0.2 M HEPES, 1.2 M KoAc, 40 mM $Mg(oAc)_2$ and 50 mM DTT at pH 7.4) was added to the homogenate. The nuclei were removed by centrifugation at 2,000 rpm for 10 min at 4 °C. The supernatant was collected and centrifuged at 16,000 *g* for 10 min at 4 °C. The supernatant (S16) was mixed with an equal volume of 1.04 M sucrose in isotonic buffer (50 mM HEPES, 100 mM KCl, 2 mM $MgCl_2$ and protease inhibitors). The solution was set at the bottom of 2.2-ml ultracentrifuge tube (Hitachi Koki, Tokyo, Japan). One milliliter of isotonic buffer was loaded onto the sucrose mixture. The tube was centrifuged at 100,000 *g* in an S55S rotor (Hitachi Koki) for 30 min at 4 °C. After the centrifugation, the LD fraction on the top of the gradient solution was recovered in isotonic buffer. The suspension was mixed with 1.04 M sucrose and centrifuged again at 100,000 *g*, as described above, to eliminate possible contamination with other organelles. The collected LD fraction was used for western blotting or the HCV RNA synthesis assay.

HCV RNA synthesis assay. An assay of HCV RNA synthesis using digitonin-permeabilized cells was performed as described previously[17]. For RNA synthesis assays using the LD fraction, the LD fraction collected by sucrose-gradient sedimentation was suspended in buffer B, which contained 2 mM manganese (II) chloride, 1 mg ml^{-1} acetylated BSA (Nacalai Tesque, Kyoto, Japan), 5 mM phosphocreatine (Sigma), 20 units/ml creatine phosphokinase (Sigma), 50 μg ml^{-1} actinomycin D, 500 μM ATP, 500 μM CTP, 500 μM GTP (Roche Diagnostics) and 1.85 MBq of [α-^{32}P] UTP (GE Healthcare, Little Chalfont, UK), and incubated at 27 °C for 4 h. The reaction products were analysed by gel electrophoresis followed by autoradiography.

Note: Supplementary Information is available on the Nature Cell Biology website.

ACKNOWLEDGEMENTS

We thank T. Fujimoto and Y. Ohsaki at Nagoya University for helpful discussions and technical assistance. Y.M. is a recipient of a JSPS fellowship. K.S. is supported by Grants-in-Aid for cancer research and for the second-term comprehensive 10-year strategy for cancer control from the Ministry of Health, Labour and Welfare, as well as by a Grant-in-Aid for Scientific Research on Priority Areas "Integrative Research Toward the Conquest of Cancer" from the Ministry of Education, Culture, Sports, Science and Technology of Japan. T.W. is also supported, in part, by a Grant-in-Aid for Scientific Research from the Japan Society for the Promotion of Science; and by the Research on Health Sciences Focusing on Drug Innovation from the Japan Health Sciences Foundation. R.B. is supported by the Sonderforschungsbereich 638 (Teilprojekt A5) and the Deutsche Forschungsgemeinschaft (BA1505/2-1). M.Z. and R.B. thank the Nikon Imaging Center at the University of Heidelberg for providing access to their confocal fluorescence microscopes and Ulrike Engel for the excellent support.

AUTHOR CONTRIBUTIONS

Y.M. and K.S. planned experiments and analyses. Y.M. was responsible for experiments for Figs 1, 2, 3a–c, 4a–e and 5b. K.A., N.U., electron microscopy; T.H., Fig. 1e; M.Z., R.B., Fig. S2e; and K.S. and K.W., Fig. 4f–g. T.W. provided JFH1 strain. Y.M. and K.S. wrote the manuscript. All authors discussed the results and commented on the manuscript.

COMPETING FINANCIAL INTERESTS
The authors declare no competing financial interests.

Published online at http://www.nature.com/naturecellbiology/
Reprints and permissions information is available online at http://npg.nature.com/reprintsandpermissions/

1. Martin, S. & Parton, R. G. Lipid droplets: a unified view of a dynamic organelle. *Nature Rev. Mol. Cell Biol.* **7**, 373–378 (2006).
2. Blanchette-Mackie, E. J. *et al.* Perilipin is located on the surface layer of intracellular lipid droplets in adipocytes. *J. Lipid Res.* **36**, 1211–1226 (1995).
3. Vock, R. *et al.* Design of the oxygen and substrate pathways. VI. structural basis of intracellular substrate supply to mitochondria in muscle cells. *J. Exp. Biol.* **199**, 1689–1697 (1996).
4. Liang, T. J. *et al.* Viral pathogenesis of hepatocellular carcinoma in the United States. *Hepatology* **18**, 1326–1333 (1993).
5. Moradpour, D., Englert, C., Wakita, T. & Wands, J. R. Characterization of cell lines allowing tightly regulated expression of hepatitis C virus core protein. *Virology* **222**, 51–63 (1996).
6. Deleersnyder, V. *et al.* Formation of native hepatitis C virus glycoprotein complexes. *J. Virol.* **71**, 697–704 (1997).
7. Kato, N. *et al.* Molecular cloning of the human hepatitis C virus genome from Japanese patients with non-A, non-B hepatitis. *Proc. Natl Acad. Sci. USA* **87**, 9524–9528 (1990).
8. Hijikata, M. & Shimotohno, K. [Mechanisms of hepatitis C viral polyprotein processing]. *Uirusu* **43**, 293–298 (1993).
9. Dubuisson, J., Penin, F. & Moradpour, D. Interaction of hepatitis C virus proteins with host cell membranes and lipids. *Trends Cell Biol.* **12**, 517–523 (2002).
10. Wakita, T. *et al.* Production of infectious hepatitis C virus in tissue culture from a cloned viral genome. *Nature Med.* **11**, 791–796 (2005).
11. Lindenbach, B. D. *et al.* Complete replication of hepatitis C virus in cell culture. *Science* **309**, 623–626 (2005).
12. Zhong, J. *et al.* Robust hepatitis C virus infection in vitro. *Proc. Natl Acad. Sci. USA* **102**, 9294–9299 (2005).
13. Pietschmann, T. *et al.* Construction and characterization of infectious intragenotypic and intergenotypic hepatitis C virus chimeras. *Proc. Natl Acad. Sci. USA* **103**, 7408–7413 (2006).
14. Moriya, K. *et al.* Hepatitis C virus core protein induces hepatic steatosis in transgenic mice. *J. Gen. Virol.* **78**, 1527–1531 (1997).
15. Hope, R. G., Murphy, D. J. & McLauchlan, J. The domains required to direct core proteins of hepatitis C virus and GB virus-B to lipid droplets share common features with plant oleosin proteins. *J. Biol. Chem.* **277**, 4261–4270 (2002).
16. Egger, D. *et al.* Expression of hepatitis C virus proteins induces distinct membrane alterations including a candidate viral replication complex. *J. Virol.* **76**, 5974–5984 (2002).
17. Miyanari, Y. *et al.* Hepatitis C virus non-structural proteins in the probable membranous compartment function in viral genome replication. *J. Biol. Chem.* **278**, 50301–50308 (2003).
18. Quinkert, D., Bartenschlager, R. & Lohmann, V. Quantitative analysis of the hepatitis C virus replication complex. *J. Virol.* **79**, 13594–13605 (2005).
19. Tauchi-Sato, K., Ozeki, S., Houjou, T., Taguchi, R. & Fujimoto, T. The surface of lipid droplets is a phospholipid monolayer with a unique fatty acid composition. *J. Biol. Chem.* **277**, 44507–44512 (2002).
20. Londos, C., Brasaemle, D. L., Schultz, C. J., Segrest, J. P. & Kimmel, A. R. Perilipins, ADRP, and other proteins that associate with intracellular neutral lipid droplets in animal cells. *Semin. Cell Dev. Biol.* **10**, 51–58 (1999).
21. Blight, K. J., McKeating, J. A. & Rice, C. M. Highly permissive cell lines for subgenomic and genomic hepatitis C virus RNA replication. *J. Virol.* **76**, 13001–13014 (2002).
22. Klein, K. C., Dellos, S. R. & Lingappa, J. R. Identification of residues in the hepatitis C virus core protein that are critical for capsid assembly in a cell-free system. *J. Virol.* **79**, 6814–6826 (2005).
23. Owsianka, A. *et al.* Monoclonal antibody AP33 defines a broadly neutralizing epitope on the hepatitis C virus E2 envelope glycoprotein. *J Virol* **79**, 11095–11104 (2005).
24. Ishii, N. *et al.* Diverse effects of cyclosporine on hepatitis C virus strain replication. *J. Virol.* **80**, 4510–4520 (2006).
25. Lohmann, V., Korner, F., Herian, U. & Bartenschlager, R. Biochemical properties of hepatitis C virus NS5B RNA-dependent RNA polymerase and identification of amino acid sequence motifs essential for enzymatic activity. *J Virol* **71**, 8416–8428 (1997).
26. Ohsaki, Y., Maeda, T. & Fujimoto, T. Fixation and permeabilization protocol is critical for the immunolabeling of lipid droplet proteins. *Histochem. Cell Biol.* **124**, 445–452 (2005).

nature
cell biology

Supplementary Figures and legends

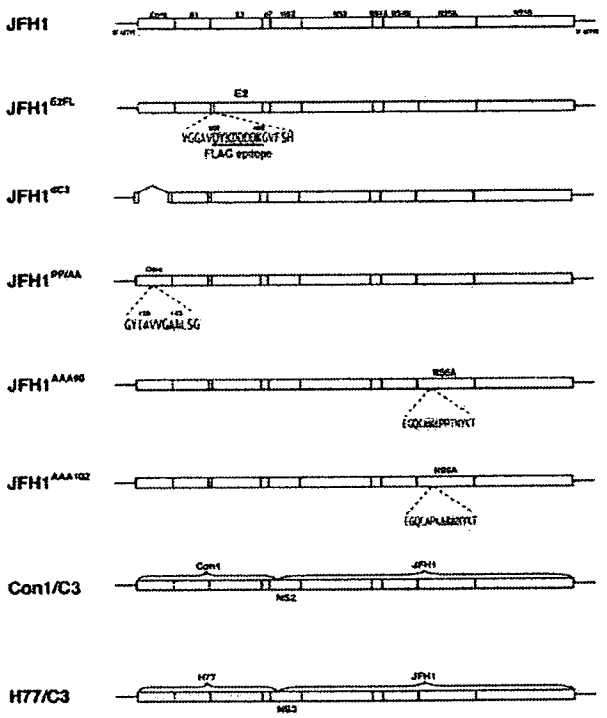

Supplementary Fig. 1

Schematic structures of HCV genomes and mutants used in this study

In JFH1^{E2FL}, the amino acid residues at positions 393 to 400 in the hyper variable region 1 of E2 were converted to a Flag epitope: DYKDDDDK. The JFH1^{E2FL} genome was used to generate other mutant variants of JFH1. In these cases the Flag epitope is marked with a blue vertical line. JFH1^{dC3} carried a deletion in the Core gene that eliminated the 17th to the 163rd amino-acid residue of Core. JFH1$^{PP/AA}$ is a mutant of JFH1^{E2FL} carrying alanine substitutions for proline residues at amino-acid positions 138 and 143 in Core. JFH1^{AAA99} and JFH1^{AAA102} contained mutated NS5A genes carrying triple-alanine substitutions for the APK sequence at amino acid positions 99 to 101 and the PPT sequence at amino acid positions 102 to 104, respectively. Constructs Con1/C3 and H77/C3 are chimeras in which the region from Core to the N-terminal domain of NS2 of JFH1 was replaced by the analogous region of the genotype 1b isolate Con1 or by the genotype 1a isolate H77[6].

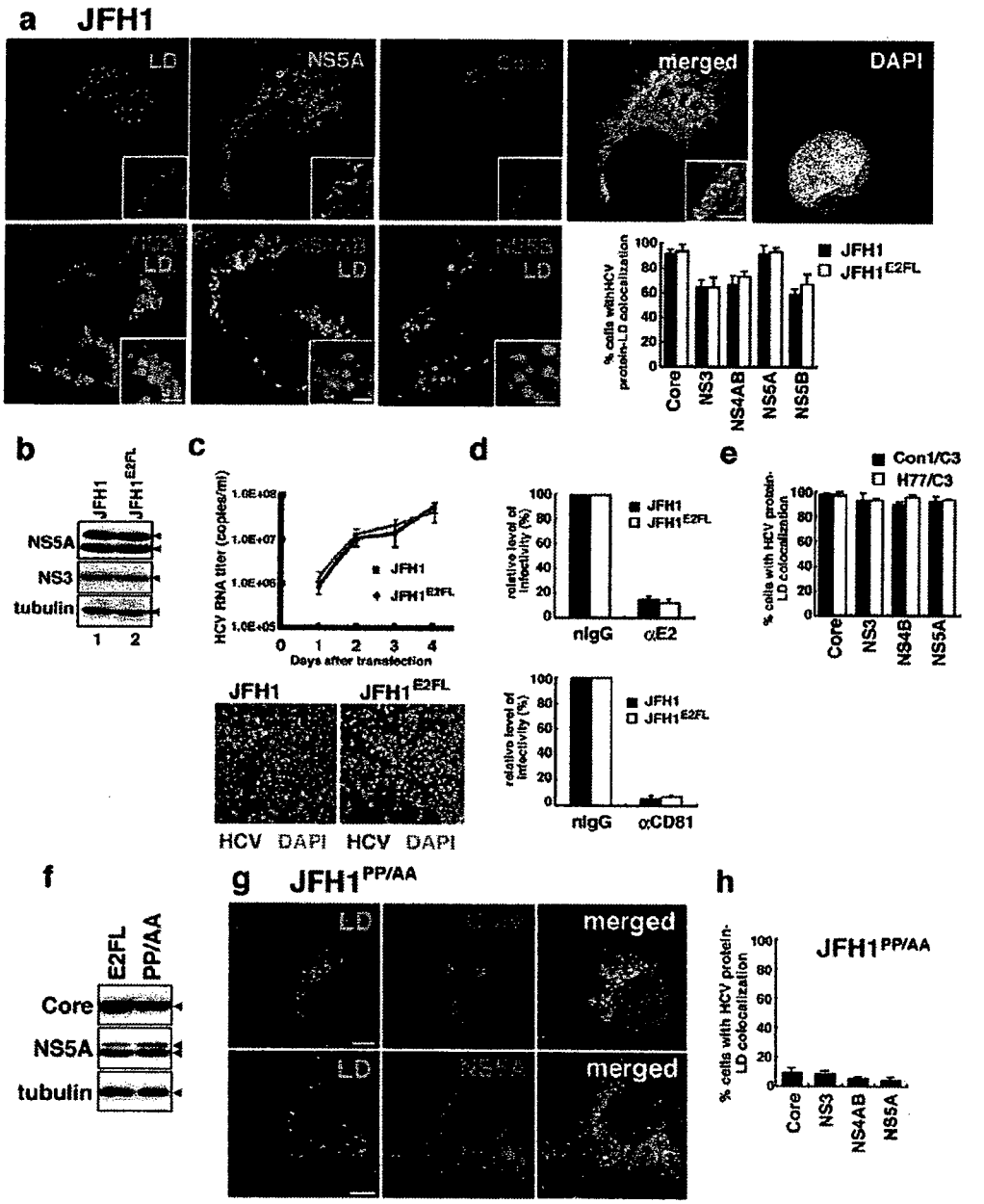

Supplementary Fig. S2 Kunitata Shimotohno
NCB-S11732B

Supplementary Fig. 2 Characterization of mutant JFH1s

(a) JFH1-replicating cells were stained with indicated antibodies, BODYPI 493/503 and

DAPI. Scale bars = 2 μm. Percentages of JFH1- and JFH1^{E2FL}-replicating cells with overlapping signals for LDs and HCV proteins (n > 200). (b) HCV proteins in JFH1 and JFH1^{E2FL} replicating cells were analyzed by western blotting with indicated antibodies. (c) Efficiency of virus production and infectivity of JFH1 and JFH1^{E2FL} viruses were analyzed as described in Fig. 4. (n = 3) (d) Inhibition of HCV infection by anti-E2 antibody and anti-CD81 antibody. JFH1 and JFH1^{E2FL} virus were pre-incubated with normal IgG (nIgG) or anti-E2 antibody for 1 hr at 4°C and were subsequently used to inoculate Huh-7.5 cells (upper panel). Huh-7.5 cells were pre-incubated with normal IgG (nIgG) or anti-CD81 antibody for 1 hr at 37°C before inoculation with JFH1 or JFH1^{E2FL} viruses (lower panel) (n = 3). No obvious difference with respect to the subcellular localization of viral proteins (a), efficiency of viral replication (b), virus production (c), and pathway of virus entry (d) were observed between JFH1^{E2FL} and JFH1 (e) Con1/C3 or H77/C3 replicating cells were stained for HCV antigens (Core or NS3 or NS4B or NS5A) and LDs. The graphs show the percentage of Con1/C3 (black) or H77/C3 (white) positive cells in which HCV protein signals overlapped with LD signals. The overlapping signals were detected by using the ImageJ RG2B software package (n > 200). (f) Whole-cell extracts of JFH1^{E2FL} (E2FL) and JFH1$^{PP/AA}$ (PP/AA) replicon-bearing cells were analyzed by Western blot with indicated antibodies. Both Core^{Wt} and Core$^{PP/AA}$ had an apparent molecular weight of about 21 kDa, indicating that Core$^{PP/AA}$ was efficiently processed. The expression level of Core$^{PP/AA}$, however, was slightly lower than that of Core^{Wt}. (g) Analysis of the subcellular localization of Core and NS5A in cells bearing the JFH1$^{PP/AA}$ mutant. Cells were labeled to detect LDs (green), Core (red), NS5A (red) and nuclei DAPI (blue). Scale bars = 10μm. (h) The percentages of JFH1$^{PP/AA}$ replicon-bearing cells positive for overlapping signals of LDs and HCV proteins are indicated (n > 200).

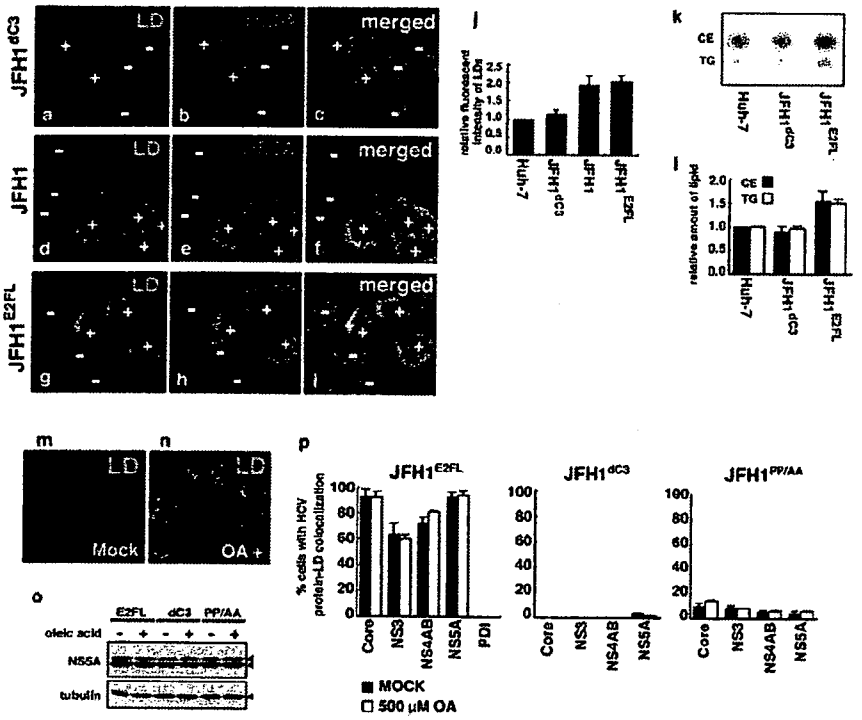

Supplementary Fig. S3 Kunitata Shimotohno
NCB-S11732B

Supplementary Fig. 3

Enhanced formation of LDs in JFH1- and JFH1^{E2FL}-replicating cells

Cells transfected with JFH1^{dC3} (a-c), JFH1 (d-f), and JFH1^{E2FL} RNA (g-i) were stained with BODIPY493/503 (green), DAPI (blue), and anti-NS5A antibody (red). + and – indicate HCV-positive and HCV-negative cells, respectively. Fluorescence intensities of LDs in Huh-7 cells, JFH1^{dC3}-, JFH1-, and JFH1^{E2FL}-replicating cells were measured by confocal microscopy. The results are represented as relative fluorescence intensity of LDs (j). (k and l) Lipid fraction extracted from Huh-7 cells, JFH1^{dC3}-, and JFH1^{E2FL}-replicating cells was analyzed by thin-layer chromatography. Each lane was loaded with lipid corresponding to an equal amount of protein. Cholesterol ester (CE) and triglyceride (TG) are indicated (k). The relative intensity of CE and TG in panel k is shown in l (n = 3). (m-p) JFH1^{E2FL} replicon-bearing cells were treated with 500 μM oleic acid for 24 hrs and were labeled with BODIPY493/503 (m and n). Cells transfected with JFH1^{E2FL} (E2FL), JFH^{dC3} (dC3), or JFH$^{PP/AA}$ (PP/AA) RNA were treated with or without oleic acid. (o) The HCV protein level as represented by the level of NS5A was analyzed by western blot. (p) The percentages of cells positive for overlapping signals for LDs and the HCV proteins or PDI are indicated. The data was obtained in the presence (500 μM) or absence (MOCK) of oleic acid in the culture medium (n > 200).

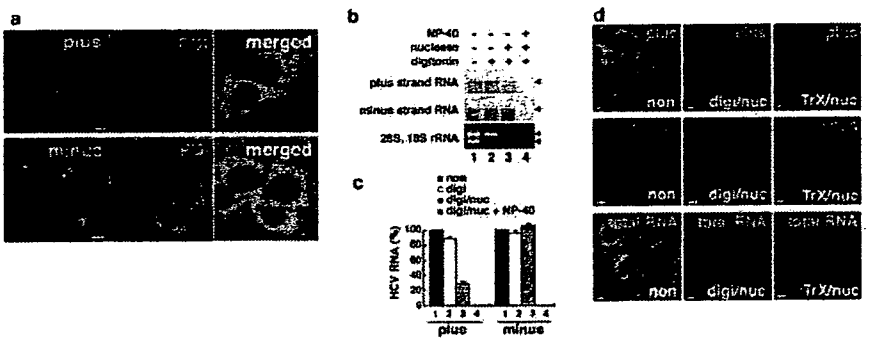

Supplementary Fig. S4 Kunitata Shimotohno
NCB-S11732B

Supplementary Fig. 4

Subcellular localizations of plus- and minus-strand HCV RNA

(a) JFH1^{E2FL} replicating cells were analyzed by *in situ* hybridization to detect plus- and minus-strand HCV RNA (green). The cells were also labeled with anti-PDI antibodies (red) and DAPI (blue). Scale bars = 10 μm. (b, c) Relative amounts of plus- and minus-strand HCV RNAs. JFH1^{E2FL}-expressing cells were permeabilized with digitonin. The cells were treated with nuclease in the presence or absence of NP-40. Then, total RNA was analyzed by Northern blots with strand-specific HCV RNA probes. 28S and 18S ribosomal RNA was stained with ethidium bromide (b). The signals were quantified and plotted in c (n = 3). The amounts of plus- and minus-strand RNA were similar before and after digitonin treatment (lanes 1 and 2). The level of plus-strand RNA, however, was reduced by approximately 70% after nuclease treatment, whereas the level of minus-strand RNA remained constant (lanes 2 and 3). Nuclease treatment in the presence of NP-40 used to lyse the membranes caused both plus- and minus-strand HCV RNA to disappear (lane 4). This result suggests that ~30% and ~100% of plus- and minus-strand HCV RNA, respectively, are located in the replication complexes. (d) Localization of nuclease-resistant JFH1^{E2FL} RNA was analyzed by *in situ* hybridization. Digitonin-permeabilized cells were treated with nuclease in the presence (TrX/nuc) or absence (digi/nuc) of Triton X-100. Total RNA was visualized with SYTO RNAselect. "non" indicates cells without digitonin and nuclease treatment. Using the nuclease-resistant HCV RNA as a marker of replication complexes, we examined the localization of the replication complexes. Both plus- and minus-strand HCV RNA were detected in the perinuclear region even after the nuclease treatment. As expected, these RNAs were no longer detectable after nuclease treatment in the presence of Triton X-100. The intensity of the plus-strand RNA signal decreased after nuclease treatment (compare upper left and middle panels). However, the intensity of the minus-strand RNA signal remained unchanged after the treatment. These results correlated with the data obtained by Northern blotting analysis. For this reason, the percentages of cells with overlapping signals for LDs and plus- or minus-strand HCV RNA (Fig. 2c) were measured after lysis of cells with digitonin and nuclease treatment. Scale bars = 10 μm.

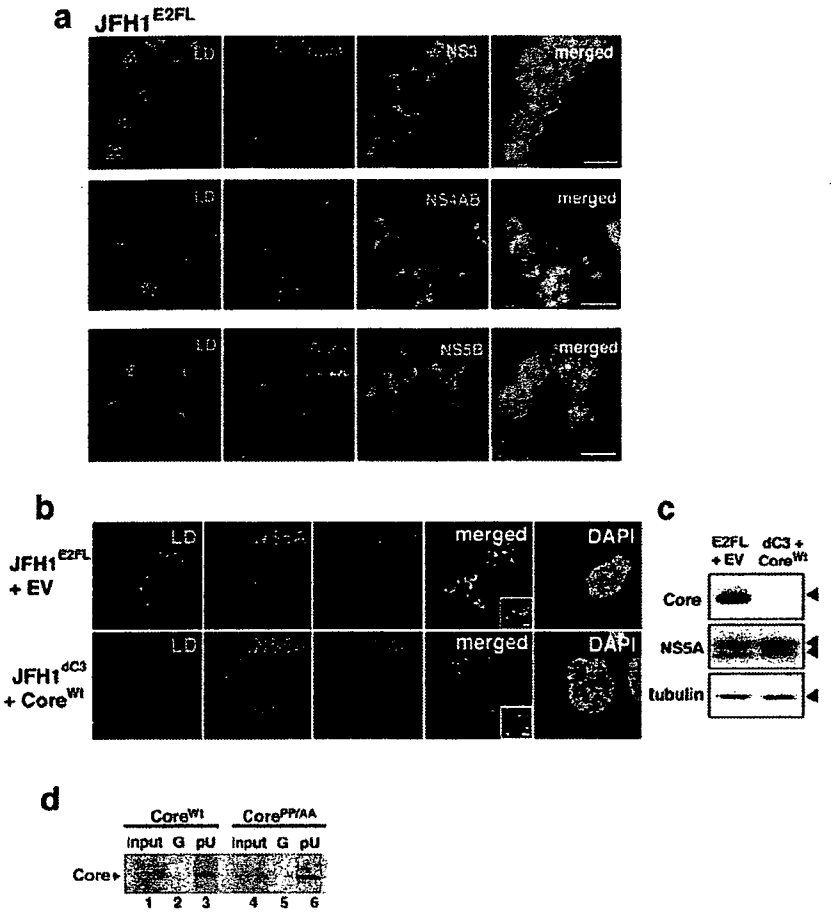

Supplementary Fig. S5 Kunitata Shimotohno
NCB-S11732B

Supplementary Fig. 5

Subcellular localization of HCV proteins in JFH1^{E2FL}-replicating cells and cells inoculated with rescued viruses, and RNA binding nature of Core.

(a) JFH1^{E2FL}-replicating cells were labeled to detect LDs (green), Core (red), NS3 (cyan), NS4AB (cyan), and NS5B (cyan). Scale bars = 2 μm **(b)** The subcellular localizations of NS5A and Core in Huh-7.5 cells infected with viruses released from JFH1^{E2FL} replicon-bearings cells co-transfected with pcDNA3 (upper panels) and from JFH1^{dC3} replicon-bearing cells co-transfected with pcDNA3-Core^{Wt} (lower panels). Cells were labeled with DAPI (white), BODIPY 493/503 (green), anti-Core (blue), and anti-NS5A (red) antibodies. The insets are high magnifications of the corresponding panel. (c) HCV proteins from these infected cells were analyzed by western blotting. (d) An RNA-protein binding precipitation assay was performed with *in vitro*-translated and ^{35}S-radiolabeled Core^{Wt} (lane 1-3) and Core$^{PP/AA}$ (lane 4-6). The resulting precipitates were analyzed by SDS-PAGE and detected by autoradiography. "G" and "pU" mark samples obtained using protein G Sepharose and poly-U Sepharose as the resin, respectively. "input" indicates 1/20 of the amount of translated product used in this assay.

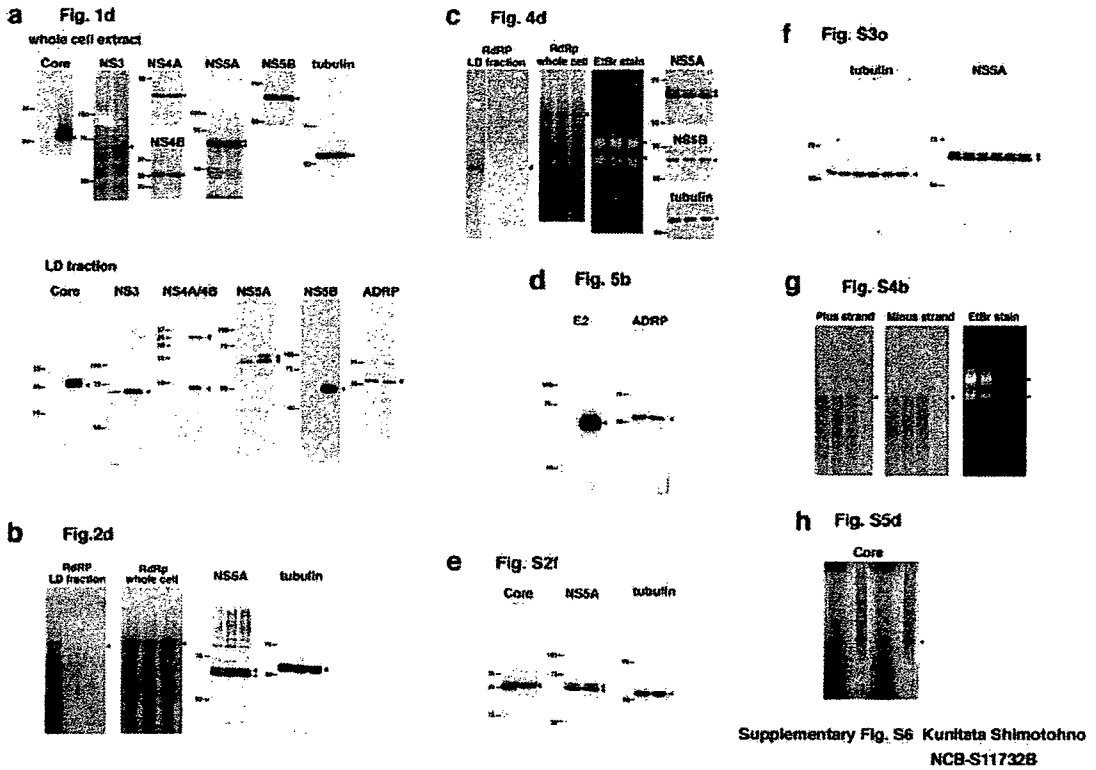

Supplementary Fig. 6

Full scan of key gel images depicted in the individual figures.

Full scans of (a) immunoblot detection of whole cell extract and LD fraction from JFH1^{E2FL}- and JFH1^{dC3}-replicating cells shown in Fig. 1d, (b) RNA synthesis assay and immunoblot detection of JFH1^{E2FL}-, JFH1^{dC3}-, and JFH1$^{PP/AA}$-replicating cells shown in Fig. 2d, (c) RNA synthesis assay and immunoblot detection of JFH1^{E2FL}-, JFH1^{AAA99}-, and JFH1^{AAA102}-replicating cells shown in Fig. 4d, (d) immunoblot detection of LD fraction from JFH1^{E2FL}- and JFH1^{dC3}-replicating cells shown in Fig. 5b, (e) immunoblot detection of JFH1^{E2FL}- and JFH1$^{PP/AA}$-replicating cells shown in Fig. S2f, (f) immunoblot detection of JFH1^{E2FL}-replicating cells shown in Fig. S3o, (g) Northern Blotting analysis of JFH1^{E2FL}-replicating cells shown in Fig. S4b, and (h) RNA-protein binding precipitation assay shown in Fig. S5d. Size of molecular weight markers (kDa) is indicated at the left side of western blot gel images. *In vitro* transcribed HCV RNA was used as a size marker for RNA gel electrophoresis (b, c, and g).

plasmid name	primer sequences (5' to 3')	template for PCR	restriction enzyme	original plasmid
pcDNA3-Core ^{1a}	AGACCCAAGCTTCACCATGAGCACAAATCCTAAACC	pJFH1	HindIII	pcDNA3
	AATGGAATTCTCAAGCAGAGACCGGAACGGTGATGC		EcoRI	
pcDNA3-TME2	AGACCCAAGCTTCACCATGGCTCAGTGGGGCGTCATGTTC	pJFH1	HindIII	pcDNA3
	AATGGAATTCTCATGCTTCCGCCTCCGCCAACAAG		EcoRI	
pcDNA3-NS3	AGACCCAAGCTTCACCATGGCTCCCATCACTGCTTATGCC	pJFH1	HindIII	pcDNA3
	AATGGAATTCTCAGGTCATGACCTCAAGGTCAGC		EcoRI	
pcDNA3-NS4B	AGACCCAAGCTTCACCATGGCCTCTAGGGCGGCTCTCATCG	pJFH1	HindIII	pcDNA3
	AATGGAATTCTCAGGATGGGATGGGGCAGTCCTC		EcoRI	
pcDNA3-NS5B	CTCGGATCCACCATGTCCATGTCATACTCCTGGACC	pJFH1	BamHI	pcDNA3
	AATGGAATTCCTACCGAGCCGGGAGTAGGAAGAGG		EcoRI	
pcDNA3-Core $^{2P/AA}$	CATGGGGTACATCGCCGTCGTAGGCGCCGCGCTTAGTGGCG	pJFH1 $^{2P/AA}$	HindIII	pcDNA3
	CGCCACTAAGCGCGGCGCCTACGAGGCGATGTAGCCCATG		EcoRI	
pJFH1 ^{E2FL}	GATTACAAGGATGACGACGATAAGGGCGTGTTCAGCCATGGCCC	pJFH1	BsiWI	pJFH1
	CTTATCGTCGTCATCCTTGTAATCAACAGCGCCTCCAACGGTGG		NotI	
	GGGACATGATGATGAACTGG			
	GTAATGTCAAACACCACACC			
pJFH1 ^{dE1}	GAAAAACCAAAAGAAACACCAACTATGCAACAGGGAACCTACC	pJFH1 ^{E2FL}	EcoRI	pJFH1 ^{E2FL}
	GTTGGTGTTTCTTTTGGTTTTTC		BsiWI	
	GGGACATGATGATGAACTGG			
	GTAATGTCAAACACCACACC			
pJFH1 $^{2P/AA}$	CATGGGGTACATCGCCGTCGTAGGCGCCGCGCTTAGTGGCG	pJFH1 ^{E2FL}	EcoRI	pJFH1 ^{E2FL}
	CGCCACTAAGCGCGGCGCCTACGAGGCGATGTAGCCCATG		BsiWI	
	GGGACATGATGATGAACTGG			
	GTAATGTCAAACACCACACC			
pJFH1 ^{E2FL} dBamHI	TACTGCCTGGCATCCTGTCTCC	pJFH1 ^{E2FL}	NsiI	pJFH1 ^{E2FL}
	GCAGACAGCATGCCACGCAGTA		BsrBI	
	GTATTAGCAATGAGGTCACC			
	GAACAATTTACACGTCAGCC			
pJFH1 ^{AAA19}	GGCCAGTGCGCGGCGGCACGCCCCACG	pJFH1 ^{E2FL}	BamHI	pJFH1 ^{E2FL} dBamHI
	CCTGCGCGGTGCCCGCCCCACTCGCC		BsrBI	
	TGGATGAACAGGCTTATTGC			
	GGTTGAAGCTCTACCTGATC			
pJFH1 ^{AAA102}	GCGCCGAAAGCCGCCGCGAACTACAAG	pJFH1 ^{E2FL}	BamHI	pJFH1 ^{E2FL} dBamHI
	CTTCTAGTTCGCCCCCCCTTTCGGCCC		BsrBI	
	TGGATGAACAGGCTTATTGC			
	GGTTGAAGCTCTACCTGATC			

Supplementary Table

A list of the plasmids used in this work. The sets of primers used to amplify the target genes, the template plasmids used in the PCRs, the restriction sites, and plasmids into which the amplified DNA fragments were inserted are shown.

Supplementary Materials and Methods

Cell culture

The human hepatoma cell lines Huh-7 and Huh-7.5[1] were grown in Dulbecco's modified Eagle's medium (DMEM; Invitrogen, CA, USA) supplemented with 10% fetal bovine serum (FBS), 100 U/ml nonessential amino acids (Invitrogen), and 100 μg/ml penicillin and streptomycin sulfate (Invitrogen). Huh-7.5 cells were obtained from Dr. C. Rice. (Rockefeller University, USA)

Plasmid construction

All plasmids were generated by insertion of PCR-amplified fragments into expression plasmids. The plasmids, the primer sequences, templates for the PCRs, and the restriction enzyme sites used to construct the plasmids are listed in Supplementary Table 1.

DNA and RNA transfection

Transfection of HCV RNA was performed as previously described[2]. DNA transfection was performed using Lipofectamine 2000 (Invitrogen) according to the manufacturer's instructions.

Northern blotting

Northern blot analysis was performed as described previously[3] with strand specific RNA probes.

RT-PCR analysis

Quantitative real-time RT-PCR analysis of the HCV RNA titer was performed as described previously[4].

ELISA for the detection of Core

Core in the culture medium was quantified with an ELISA according to the manufacturer's protocol (HCV antigen ELISA test, Ortho-Clinical Diagnostics).

Thin-layer chromatography

Lipid samples extracted from cells were dissolved in chloroform methanol and were

subjected to thin-layer chromatography with a high-performance TLC plate (Merck) by the two-step method[5]. The plate was charred by a copper acetate phosphoric acid solution at 180°C.

***In vitro* transcription**

RNA for transfection was synthesized using MEGAscript T7 (Ambion, TX, USA). Plasmids carrying the JFH1 RNA sequence were linearized with *Xba*I and used as templates for transcription. Probes for *in situ* hybridization were synthesized using MAXIscript Sp6 or T7 (Ambion) in the presence of the DIG RNA labeling mix (Roche). Probes for Northern blots were synthesized with MAXIscript Sp6 or T7 in the presence of 1.85 MBq of [α-^{32}P] UTP (Amersham Biosciences). For detection of plus-strand HCV RNA, minus-strand RNA probes were generated using pcDNA3-TME2 (*Hin*dIII for linearization), pcDNA3-NS3 (*Hin*dIII), and pcDNA3-NS5B (*Bam*HI) as templates for *in vitro* transcription. For detection of minus-strand HCV RNA, plus-strand RNA probes were generated using pcDNA3-TME2 (*Eco*RI), pcDNA3-NS3 (*Xba*I), and pcDNA3-NS5B (*Bam*HI) as templates. The RNA probes used for *in situ* hybridization were subjected to alkaline hydrolysis to generate fragments of ~170 nucleotides in length. Synthesized RNA probes were treated with DNase I (Ambion) and size fractionated using MicroSpin G-50 columns (Amersham Biosciences).

Sucrose density gradient centrifugation of culture medium

The 100-time concentrated medium from JFH1-bearing cells was loaded onto 20-50% [w/v] sucrose gradient containing 50 mM Hepes-KOH (pH 7.4), 100 mM NaCl and 1mM EDTA followed by centrifugation at 100,000 x g for 16 hrs using RPS40T rotor of HITACHI ultracentrifuge. The gradient was fractionated into 31 fractions. Buoyant density of each fraction was analyzed by Abe refractometer (ATAGO Inc., Japan). Each fraction was dialyzed against serum free DMEM and was used for the infection experiment as well as quantification of Core and HCV RNA titer as described above.

Infection experiments

Cells were cultured in DMEM containing 5% FBS. The medium was collected and mixed with a 0.01 volume of 1 M HEPES (pH 7.4). After filtering the sample through a 0.22-μm filter (Millipore), the filtrate was concentrated by reducing the volume to

between 1/50 and 1/100 of the original volume with an Amicon Ultra-15 centrifugal filter with Ultracel-100 membrane (Millipore). Huh-7.5 cells seeded on a collagen-coated Labtech II 8-well chamber were incubated with 100 μl of the concentrated medium for 120 min. Then, the cells were washed three times with DMEM. Twenty-four hours after the inoculation, the cells were labeled with serum from HCV-infected patients to determine the infectivity level.

***In situ* hybridization analysis**

Huh-7 cells transfected with JFH1 RNA were seeded on a collagen-coated Labtech II 8-well chamber (Nunc). Three days after seeding, the cells were washed twice with PBS and fixed with fixation solution for 15 min at room temperature. Then, the cells were permeabilized with 0.05% Triton X-100 in fixation solution for 15 min at room temperature. After washing the cells twice with cold DEPC-treated PBS, the cells were incubated in 95% formamide and 0.1x SSC (1x SSC: 150 mM NaCl and 15 mM sodium citrate) for 15 min at 65°C. After chilling the chamber on ice, the cells were incubated in 100 μl of pre-hybridization solution for 60 min at room temperature. Pre-hybridization solution was composed of 50% formamide, 2x SSC, 1 μg/ml of salmon sperm DNA (sonicated to 1-2 kb pieces, Roche), 1 μg/ml of yeast tRNA (Roche), and 2 mM vanadyl ribonucleoside complex (NEB). Then, the cells were incubated in 100 μl of hybridization solution (pre-hybridization solution containing 10% dextran sulfate and 100 to 500 ng/ml of the RNA probes) for 40 hrs at 42°C. After the hybridization, the slide glass in the chamber was transferred to a bucket filled with wash solution 1 (50% formamide and 2x SSC at pH 7.4) and washed three times for 20 min at 50°C with gentle agitation. Then, the slide was washed three more times in wash solution 2 (0.1x SSC at pH 7.4) for 20 min at 50°C with gentle agitation. The slide was incubated in blocking solution for 30 min at room temperature. To detect DIG-labeled probes, sheep anti-DIG antibodies (Roche) and Alexa 488 or Alexa 568 anti-sheep IgG antibodies (Invitrogen) were used as primary and secondary antibodies, respectively. When HCV RNA, Core, and NS5A were simultaneously labeled in the same sample, anti-DIG antibodies and the Alexa-conjugated antibodies were incubated with the samples separately to avoid cross-reaction of the Alexa 488 or Alexa 568 anti-sheep IgG antibodies with mouse and rabbit IgG. Briefly, the incubation with the anti-DIG antibodies and the Alexa 488 anti-sheep IgG antibodies was performed first. After

washing with PBS followed by a second fixation procedure, the cells were incubated with anti-Core and anti-NS5A antibodies followed by Alexa 568 anti-rabbit IgG and Alexa 647 anti-mouse IgG antibodies. For treatment with nuclease, digitonin-permeabilized cells were treated with 1 μg/ml of RNase A in the presence or absence of 0.05% Triton X-100 for 15 min at 37°C. After the treatment, RNase A was inactivated by incubation with 4% formaldehyde. Then, the cells were completely permeabilized with 0.05% Triton X-100 for 5 min at room temperature.

Statistical analysis of the recruitment of viral components to the LD

Only the cells that have any LDs surrounded by HCV proteins, PDI, or HCV RNA were counted as positive under immunofluorescence microscopy, and those adjacent to HCV signal were not included. The obtained cell number was divided by the total number of HCV replicating cells and is shown as "% cells with HCV protein-LD colocalization". In case of the chimeras Con1/C3 and H77/C3 LD colocalization with HCV proteins was additionally analyzed by using the ImageJ RG2B software package (Rasband, W.S., ImageJ, U. S. National Institutes of Health, Bethesda, Maryland, USA, http://rsb.info.nih.gov/ij/, 1997-2006.). Approximately 200 cells were examined for each antigen.

RNA-protein binding precipitation assay

In vitro translated [^{35}S]-labeled products (Core^{Wt} and Core$^{PP/AA}$) were incubated with poly-U or protein G Sepharose resin in 50 mM HEPES (pH7.4), 100 mM NaCl, 0.1 % NP-40, and RNase inhibitor at 4°C for 2 hrs. After five washes, resin-bound radiolabeled proteins were analyzed by gel electrophoresis followed by autoradiography.

Supplementary References

1. Blight, K. J., McKeating, J. A. & Rice, C. M. Highly permissive cell lines for subgenomic and genomic hepatitis C virus RNA replication. *J Virol* **76**, 13001-14 (2002).
2. Lohmann, V. et al. Replication of subgenomic hepatitis C virus RNAs in a hepatoma cell line. *Science* **285**, 110-3 (1999).
3. Miyanari, Y. et al. Hepatitis C virus non-structural proteins in the probable membranous compartment function in viral genome replication. *J Biol Chem* **278**, 50301-8 (2003).
4. Takeuchi, T. et al. Real-time detection system for quantification of hepatitis C virus genome. *Gastroenterology* **116**, 636-42 (1999).
5. Tauchi-Sato, K., Ozeki, S., Houjou, T., Taguchi, R. & Fujimoto, T. The surface of lipid droplets is a phospholipid monolayer with a unique Fatty Acid composition. *J Biol Chem* **277**, 44507-12 (2002).
6. Pietschmann, T. et al. Construction and characterization of infectious intragenotypic and intergenotypic hepatitis C virus chimeras. *Proc Natl Acad Sci U S A* **103**, 7408-13 (2006).

Journal of General Virology (2007), **88**, 2495–2503 DOI 10.1099/vir.0.82872-0

Robust production of infectious viral particles in Huh-7 cells by introducing mutations in hepatitis C virus structural proteins

David Delgrange,[1] André Pillez,[1] Sandrine Castelain,[1,2] Laurence Cocquerel,[1] Yves Rouillé,[1] Jean Dubuisson,[1] Takaji Wakita,[3] Gilles Duverlie[1,2] and Czeslaw Wychowski[1]

Correspondence
Czeslaw Wychowski
czeslaw.wychowski@ibl.fr

[1]CNRS-UMR 8161, IBL, Université de Lille I et Lille II, Institut Pasteur de Lille, 59021 Lille cedex, France

[2]Laboratoire de Virologie, Centre Hospitalier Universitaire-Hôpital Sud, 80054 Amiens cedex, France

[3]Department of Virology II, National Institute of Infectious Diseases, 1-23-1 Toyama, Shinjuku, Tokyo 162-8640, Japan

Recently, the characterization of a cell culture system allowing the amplification of an authentic virus, named hepatitis C virus cell culture (HCVcc), has been reported by several groups. To obtain higher HCV particle productions, we investigated the potential effect of some amino acid changes on the infectivity of the JFH-1 isolate. As a first approach, successive infections of naïve Huh-7 cells were performed until high viral titres were obtained, and mutations that appeared during this selection were identified by sequencing. Only one major modification, N534K, located in the E2 glycoprotein sequence was found. Interestingly, this mutation prevented core glycosylation of E2 site 6. In addition, JFH-1 generated with this modification facilitated the infection of Huh-7 cells. In a second approach to identify mutations favouring HCVcc infectivity, we exploited the observation that a chimeric virus containing the genotype 1a core protein in the context of JFH-1 background was more infectious than wild-type JFH-1 isolate. Sequence alignment between JFH-1 and our chimera, led us to identify two major positions, 172 and 173, which were not occupied by similar amino acids in these two viruses. Importantly, higher viral titres were obtained by introducing these residues in the context of wild-type JFH-1. Altogether, our data indicate that a more robust production of HCVcc particles can be obtained by introducing a few specific mutations in JFH-1 structural proteins.

Received 23 January 2007
Accepted 1 May 2007

INTRODUCTION

The *Hepatitis C virus* (HCV) is the only member of the genus *Hepacivirus* of the family *Flaviviridae*. HCV is a major cause of chronic hepatitis, liver cirrhosis, hepatocellular carcinoma (Major *et al.*, 2001) as well as several extrahepatic diseases (Houghton, 1996). An estimation of about 170 million people infected with HCV worldwide has been reported (Poynard *et al.*, 2003; Thomas, 2000).

HCV is an enveloped single-strand, positive-sense RNA virus and its genome encodes a unique open reading frame that is flanked by two structured non-translated regions in 5′ and 3′ ends of HCV genome (5′NTR and 3′NTR). Mediated by an internal ribosome entry site (Tsukiyama-Kohara *et al.*, 1992), the translation of HCV RNA genome results in polyprotein synthesis that is processed by cellular and viral proteases into at least 10 structural and non-structural (NS) proteins (Grakoui *et al.*, 1993; Hijikata *et al.*, 1991). In the viral particle, HCV genomic RNA is complexed with the highly basic capsid protein. On its surface, the viral particle bears two envelope glycoproteins E1 and E2 that are anchored in the lipid bilayer. Both these proteins have been shown to accumulate in the endoplasmic reticulum (ER), where the particles are probably assembled (Op De Beeck *et al.*, 2001). A small integral membrane protein, p7, has been reported to function as an ion channel (Griffin *et al.*, 2003; Pavlovic *et al.*, 2003). Among the NS proteins NS2, NS3, NS4A, NS4B, NS5A and NS5B, which coordinate the intracellular processes of the virus life cycle, only proteins NS3 through to 5B are sufficient to support the HCV RNA replication (Lohmann *et al.*, 1999). In addition to the polyprotein, a new HCV protein with an unknown function has also been reported. The so-called F-protein (frameshift) or ARFP (alternative reading frame protein) is generated by ribosomal frameshifting into an alternative reading frame within the

capsid-coding sequence (Roussel *et al.*, 2003; Varaklioti *et al.*, 2002; Walewski *et al.*, 2001; Xu *et al.*, 2001).

Despite intensive research efforts, the HCV life cycle and host–virus interactions have been difficult to investigate due to the lack of efficient cell culture and small animal models. Nevertheless, significant progress has been made by using heterologous expression systems. Infectivity of some cDNA-derived HCV RNAs has been demonstrated in chimpanzees upon intrahepatic inoculation (Kolykhalov *et al.*, 1997; Yanagi *et al.*, 1997, 1999). Also, the development of a functional cell-based replication system allowing efficient replication of HCV subgenomic RNAs (replicons) has provided an important tool for studying the HCV RNA replication or for evaluating potential antiviral compounds (Blight *et al.*, 2000; Lohmann *et al.*, 1999). Several surrogate systems have also been developed to palliate the difficulties in studying interactions between several candidate HCV receptors and the HCV glycoproteins. Thus, retrovirus-based pseudoparticles (pp) or HCVpp has provided the first insight into HCV entry (Bartosch *et al.*, 2003; Hsu *et al.*, 2003). But the major breakthrough arose recently with the propagation of virus in a human liver hepatoma cell line, Huh-7 (Wakita *et al.*, 2005), by transfecting these cells with an RNA transcribed from a full-length cDNA cloned initially from a patient with a fulminant hepatitis and infected with a genotype 2a isolate (Kato *et al.*, 2001). Unfortunately, it was reported by this group that the efficacy of the infection was low. Subsequently, different papers reported a robust production of infectious virus obtained with a homologous chimeric FL-J6/JFH-1 (Lindenbach *et al.*, 2005) or obtained into Huh-7.5.1 cells (Zhong *et al.*, 2005), derived from a cell line (Huh-7.5) having a defect in the RIG-I pathway (Sumpter *et al.*, 2005).

In this study, a highly efficient *in vitro* infection system based on Huh-7 cell line was obtained. The transcribed genomic JFH-1 RNA was used to produce infectious virus. The viral titre was initially low; however, successive infections of naïve Huh-7 cells led to a robust production of virus. The sequencing of the viral genome revealed only a few mutations located in the E2 glycoprotein. Furthermore and based on the characterization of a 1a–2a chimeric virus, we showed by site-directed mutagenesis that 2 aa present in the C-terminal part of the capsid-coding sequence were important for the production of high titres. Consequently, a robust HCV particle production was obtained independently of the Huh-7.5.1 cells or JFH-1 recombinant viral genome.

METHODS

Cell culture. Cell monolayers of human hepatoma cell line Huh-7 (Nakabayashi *et al.*, 1982) were grown in Dulbecco's modified essential medium (DMEM; Invitrogen) supplemented with 100 nmol non-essential amino acids l^{-1} and 10 % fetal bovine serum (FBS).

Antibodies. Rat monoclonal antibody (mAb) 3/11 (Flint *et al.*, 1999), kindly provided by J. McKeating (Institute of Biomedical Research, Birmingham University, UK) was produced *in vitro* by using a MiniPerm apparatus (Heraeus) as recommended by the manufacturer. Anti-C (ACAP27) mouse mAb was kindly provided by J. F. Delagneau (Bio-Rad, Marne-La-Coquette 92430, France). Anti-E2 mouse mAb AP33 was kindly provided by A. Patel (MRC Virology Unit, Institute of Virology, Glasgow, UK). Goat anti-β-actin polyclonal antibodies were from Santa Cruz. Alexa 488-conjugated and Alexa 555-conjugated goat anti-mouse secondary antibodies were from Molecular Probes.

Plasmid construction. The plasmids pJFH-1 containing the full-length cDNA of JFH-1 isolate, belonging to subtype 2a (GenBank accession no. AB047639), pJFH-1/GND and pJFH-1/ΔE1-E2 were described previously (Wakita *et al.*, 2005). Individual or combined viral mutations N534K (N6), F172C and P173S (FP→CS) were introduced into the pJFH-1 plasmid by sequential PCR steps as described using the high fidelity deep vent DNA polymerase (New England Biolabs), then assembled by a second PCR amplification (Goffard *et al.*, 2005), followed by restriction digestions and ligation. The resulting plasmids were named pJFH-1/N6 (N534K) and pJFH-1/CS. The plasmid pJFH-1/CS-N6 was obtained by inserting the fragment *BsiW1–NotI* obtained from pJFH-1/N6 into the plasmid pJFH-1/CS. All constructs were verified by DNA sequencing.

***In vitro* transcription.** To generate genomic HCV RNA, the plasmid pJFH-1 and derivatives were linearized at the 3′ end of the HCV cDNA with the restriction enzyme *Xba*I (New England Biolabs). Following treatment with Mung Bean Nuclease, the linearized DNAs were then precipitated overnight and resuspended in RNase-free water to a concentration of 1 $\mu g\ \mu l^{-1}$. *In vitro* transcripts were generated using Megascript (Ambion) according to the manufacturer's protocol. The *in vitro* reaction was set up and incubated at 37 °C for 4 h. To degrade the DNA template, DNase I was added and incubated for another 20 min at 37 °C. The *in vitro* transcripts were then precipitated by the addition of LiCl and the precipitates were recovered by centrifugation. The concentration of each transcript was determined by measurement of the absorbance at 260 nm. *In vitro* transcribed RNA was delivered to cells by electroporation as described previously (Kato *et al.*, 2003a). Viral stocks were obtained by harvesting cell culture supernatants at 1 week post-transfection. Secondary viral stocks were obtained by additional infections of naïve Huh-7 cells.

Successive infections and titration of HCV RNA by RT-PCR. Huh-7 cells were seeded at 7×10^5 cells in T25 flask and inoculated with 2 ml supernatant medium from cells transfected with the infectious JFH-1 RNA. At 24 h, the cells were supplemented with 4 ml complete DMEM. At day 3 post-infection, infected cells were trypsinized and then replated at 2×10^6 cells in a T75 flask. Indirect immunofluorescence was used to estimate the levels of infectivity of the amplified virus. In addition, for quantification of HCV RNA, the RNA was extracted from the supernatant of infected cells and titrated by quantitative real-time RT-PCR assay (RT-qPCR) (Castelain *et al.*, 2004).

HCV RNA genome sequencing. Five microlitre aliquots of the RNA solutions were subjected to reverse transcription with random hexamer and moloney murine leukemia virus reverse transcriptase (Superscript II; Invitrogen) at 42 °C for 1 h. PCR primers of 20-mer designated on the sequence of JFH-1 were used to amplify five fragments of HCV cDNA (nt 129–626, 467–2367, 2285–4665, 4594–7003 and 6950–9634) to cover most of the HCV genome. One microlitre of the cDNA was subjected to PCR with TaKaRa LA *Taq* polymerase (Takara Biochemicals), and PCR conditions consisted of 30 cycles each with a denaturing cycle at 95 °C for 30 s, an annealing cycle at 60 °C for 30 s and an extension cycle at 72 °C for 2 min. The sequence of each amplified DNA was determined.

Titration of HCV cell culture (cc). Huh-7 cells were seeded at 8×10^4 cells per well in a 24-well plate. The next day, cell supernatants of transfected or infected Huh-7 cells were serially diluted in DMEM and used to infect naïve Huh-7 cells. The inoculum was incubated for 2 h at 37 °C, washed with DMEM and then overlaid with complete DMEM. The viral titre was then determined at 3 days post-infection by indirect immunofluorescence staining of the capsid protein and expressed as focus-forming unit per millilitre (f.f.u. ml^{-1}) as described previously (Zhong *et al.*, 2005).

Western blot analysis. Cells were lysed in a buffer containing 50 mM Tris/HCl (pH 7.5), 150 mM NaCl, 5 mM EDTA, 0.5 % (v/v) Igepal and a mixture of protease inhibitors (Complete; Roche). Protein content of pre-cleared cell lysates was determined by the BCA method as recommended by the manufacturer (Sigma), using BSA as a standard. Total proteins were separated by SDS-PAGE, transferred to nitrocellulose membranes (Hybond-ECL; Amersham) by using a Trans-Blot apparatus (Bio-rad) and revealed with a specific mAb followed by goat anti-mouse or anti-rat IgG conjugated to peroxidase (Jackson Immunoresearch) and donkey anti-goat conjugated to peroxidase. The immune complexes were visualized by enhanced chemiluminescence detection (ECL; Amersham) as recommended by the manufacturer.

Indirect immunofluorescence microscopy. Infected Huh-7 cells grown on coverslips were fixed in 4% paraformaldehyde. Immunostaining was performed as described previously (Rouille *et al.*, 2006) using anti-C ACAP27 mouse mAbs and anti-E2 3/11 rat mAb, followed by species-specific-conjugated secondary antibodies. Image acquisition was carried out using an Axiophot 2 microscope (Zeiss) equipped with a camera. For confocal microscopy, double-label staining was performed with anti-E2 mouse mAb AP33 (IgG1) and anti-C mouse mAb ACAP27 (IgG2a) followed by Alexa 488-conjugated goat anti-mouse IgG2a and Alexa 555-conjugated goat anti-mouse IgG1. Fluorescent signals were collected with a Leica SP2 confocal microscope equipped with a PL APO × 100/1.4 immersion objective.

RESULTS

Production of infectious virus in Huh-7 cell line by a transcribed genomic JFH-1 RNA

In an attempt to generate higher infection titres for HCV, Huh-7 cells were electroporated with an *in vitro* transcribed genomic JFH-1 RNA (Wakita *et al.*, 2005). Transfected cells were then passaged every 5–7 days in order to maintain subconfluent cultures during the experiment. Immunofluorescence staining for capsid and E2 proteins revealed that the percentage of positive cells increased from 30% at day 2 to 80% at day 12, after two passages (Fig. 1a). These results suggest that the virus spread within the cell culture allowing the untransfected cells to be infected. Western blot analyses of transfected cells showed that the capsid and E2 proteins were still detected after 33 days (Fig. 1b) and even after 90 days (data not shown). Similar results were obtained for NS3 (data not shown). Virus released in the supernatant of transfected cells was then used to inoculate naïve Huh-7 cells. Immunofluorescence staining revealed that a low percentage of cells was positive (Fig. 1c), but after several passages, all cells were infected (data not shown). Controls for transfection and infection were also performed with JFH-1/ΔE1-E2 and JFH-1/GND. No infection was observed with these constructs as described previously (data not shown) (Wakita *et al.*, 2005). Titration of HCV RNA by RT-qPCR assay revealed that after the first passage of transfected cells the level of detection of HCV RNA was low (Table 1). However, the extracellular HCV RNA increased slowly in the supernatant of transfected cells reaching a maximal level of 2×10^6 genome equivalent (GE) ml^{-1} after four passages (P_4). In the same time, the infectious viral titre was only approximately 10^3 f.f.u. ml^{-1}. These results indicate that our Huh-7 cells can replicate JFH-1 RNA and can be infected with HCV particles. However, in transfected cells maintained in culture, the production of infectious viral particles remained low.

Increase in HCVcc infectivity after several rounds of infection

As a first approach, successive infections of naïve Huh-7 cells were performed to obtain higher titres of infectious virus. The scheme of infection is presented in Fig. 2. To follow the release of infectious virus particles in the supernatant, the viral RNA was extracted from supernatant and titrated by RT-qPCR. The successive infections, performed on Huh-7 cells with JFH-1 (noted I_1–I_6), led to a progressive release of viral genomes in the supernatant of inoculated cells, which reached a maximal level of 2.9×10^8 GE ml^{-1} after six successive infections (Table 1). Substantially more viral RNA was released into supernatant fluids of infected cells in I_5 or I_6 than in transfected cells. Interestingly, infectious titres ranging between 10^5 and 10^6 f.f.u. ml^{-1} were obtained at I_5 and I_6, indicating that a robust infection could be obtained with Huh-7 cell line after successive infections.

Identification of mutations in the JFH-1 virus produced in I_6

Since a highly infectious JFH-1 virus was obtained after several passages, we wanted to define whether some mutations were selected during the successive infections of Huh-7 cells. To identify potential mutations in JFH-1 isolate, total cellular RNAs were prepared from infected cells in I_6 and the full HCV RNA genome was sequenced by RT-PCR. This approach should allow us to determine the major modifications selected during the successive infections. Surprisingly, the sequencing revealed the presence of only three mutations that were located in the E2-coding sequence. Two of them were silent mutations found at positions 1843 and 1912 (G→A and U→C). The third mutation, at position 1942 (U→A), led to a change in amino acid from Asn 534 to a Lys (N534K), which is a potential site of *N*-glycosylation (N6 site) (Fig. 3a). Thus, to verify that the core glycosylation was modified in E2 of JFH-1 produced in I_6, the E2 glycoprotein resulting of the first transfection was compared with that resulting of the last infection (I_6). As confirmed by immunoblotting, a slight shift in the E2 migration was observed (Fig. 3b, lanes I_6 and wt). Furthermore, no differences in the migration